Modeling of Cylindrical Pin-Fin Heat Sinks for Electronic Packaging

W. A. Khan, J. R. Culham, and M. M. Yovanovich
Microelectronics Heat Transfer Laboratory
Department of Mechanical Engineering
University of Waterloo
Waterloo, Ontario, Canada N2L 3G1
Email: wkhan@mhtlab.uwaterloo.ca

Abstract

Analytical models are presented for determining heat transfer from in-line and staggered pin-fin heat sinks used in electronic packaging applications. The heat transfer coefficient for the heat sink and the average temperature for the fluid inside the heat sink are obtained from an energy balance over a control volume. In addition, friction coefficient models for both arrangements are developed from published data. The effects of thermal conductivity on the thermal performance are also examined. All models can be applied over a wide range of heat sink parameters and are suitable for use in the design of pin-fin heat sinks. The present models are in good agreement with existing experimental/numerical data.

Nomenclature

A	=	area $[m^2]$
c_p	=	specific heat of fluid, $J/kg \cdot K$
D	=	pin diameter $[m]$
f	=	friction factor
H	=	pin height $[m]$
h	=	heat transfer coefficient $[W/m^2K]$
K_1	=	correction factor
k	=	thermal conductivity $[W/mK]$
k_c	=	coefficient of contraction
k_e	=	coefficient of expansion
L	=	length of heat sink in flow direction $[m]$
m	=	fin performance parameter $[m^{-1}]$
$\dot{m}$	=	mass flow rate of air $[kg/s]$
N	=	total number of pins in heat sink $\equiv N_T N_L$
N_L	=	number of rows in streamwise direction
N_T	=	number of rows in spanwise direction
Nu_D	=	Nusselt number based on pin diameter
Pr	=	Prandtl number $\equiv c_p\mu/k$
Q	=	heat flow rate $[W]$
R	=	resistance $[^0C/W]$
Re_D	=	Reynolds number $\equiv DU_{max}/\nu$
$\mathcal{S}_D$	=	dimensionless diagonal pitch $\equiv S_D/D$
$\mathcal{S}_L$	=	dimensionless streamwise pitch $\equiv S_L/D$
$\mathcal{S}_T$	=	dimensionless spanwise pitch $\equiv S_T/D$
S_D	=	diagonal pitch $[m]$
S_L	=	pin spacing in streamwise direction $[m]$
S_T	=	pin spacing in spanwise direction $[m]$
T	=	absolute temperature $[K]$
t	=	thickness $[m]$
U	=	velocity of air $[m/s]$
W	=	width of heat sink $[m]$

Greek

ΔP	=	pressure drop $[Pa]$
γ	=	slenderness ratio $\equiv H/D$
μ	=	absolute viscosity of fluid $[kg/m\,s]$
ν	=	kinematic viscosity of fluid $[m^2/s]$
ρ	=	fluid density $[kg/m^3]$

Subscripts

app	=	approach
a	=	ambient
b	=	exposed surface of base plate
max	=	max
w	=	wall
f	=	fluid
fin	=	single fin
hs	=	heat sink
m	=	bulk material

1. Introduction

Heat sinks are the most common thermal management hardware used in micro- and opto-electronics. They improve the thermal control of electronic components, assemblies, and modules by enhancing their surface area through the use of pin-fins. Applications utilizing pin-fin heat sinks for cooling of electronics have increased significantly during the last few decades due to an increase in heat flux densities and product miniaturization. To the author's knowledge, no analytical/experimental/numerical work exists for the fluid friction for pin-fin heat sinks. However, many experimental/numerical studies regarding flow across tube banks exists in literature. Due to similarities between the geometry of a heat exchanger tube bundle and pin-fin arrays, previous work related to tube banks provides some guidance in modeling fluid flow in pin-fin heat sinks.

1.1 Previous Work

Chilton and Genereaux [1], Grimison [2], Jakob [3], and Gunter and Shaw [4] reviewed the existing data obtained by a number of authors including Bergelin et. al [5], Norris and Spofford [6], Huge [7], Pierson [8],

0-7803-8985-9/05/$20.00 ©2005 IEEE

and Wallis and White [9] on the pressure drop across tube banks and proposed different correlations of friction factors for both in-line and staggered arrangements in terms of Reynolds numbers. Žukauskas and Ulinskas [10] recommended more than 30 empirical correlations for friction factors based on arrangement, Reynolds number and longitudinal and transverse pitches. In this study, these correlations are fitted to give simple correlations for each arrangement in terms of $\mathcal{S}_\mathcal{T}$, $\mathcal{S}_\mathcal{L}$, and Re_D.

Dvinsky et. al [11], Jung and Maveety [12], You and Chang [13], Wang and Sangani [14], and Wung and Chen [15] performed numerical studies to model the heat transfer characteristics of pin-fin array heat exchangers. Some authors proposed Nusselt number correlations for a limited range of configurations and Reynolds numbers.

Tahat et. al [16, 17], Maudgal and Sunderland [18], Wirtz et. al [19], Babus'Haq et. al [20], Azar and Mandrone [21], and Minakami and Iwasaki [22] performed experimental studies and proposed empirical correlations. Van Fossen [23] and Metzger et al. [24 - 26] have done similar but independent studies of short pin-fin arrays with various aspect ratios and spacings for the staggered array. Armstrong and Winstanley [27] presented a review of works specifically on short pin fin arrays. They showed that not only is the existence of an active bounding wall a significant departure from the classical tube bundle situations, but also that the heat transfer from the pins themselves is lower than from long pin fins/cylinders. Hamilton et al. [28] used a 3-D finite element based numerical simulation to model the heat transfer characteristics of a staggered short pin-fin array heat exchanger. The simulation was validated against available experimental data, and then used to estimate overall array averaged heat transfer coefficient and pressure drop for various pin-fin configurations and Reynolds numbers. They proposed a correlation similar in form as by Grimisom [2] and Žukauskas and Ulinskas [10] for a limited range of configurations and Reynolds numbers. Their correlation works only for $3500 < Re_{Dmax} < 14000$.

Several other empirical models of heat transfer from tube banks in crossflow have also been reported in the literature. Grimisom [2] and Žukauskas and Ulinskas [10] are the main contributors in this regard. Their models are available in tabular form in many heat transfer text books (Holman [29], Kreith [30] and Incropera and DeWitt [31]. It is important to note that all those models were developed for a specific fluid, longitudinal and transverse pitches, Reynolds and Prandtl numbers. The user can not extrapolate those correlations over a wide range of operating conditions often found in existing heat exchangers. Those correlations lead to unrealistic predictions, discontinuities and numerical difficulties if they are used outside the range for which they were developed. In order to avoid these problems new comprehensive models are developed that can be used for a wide range of parameters discussed above. In developing these models, it is assumed that the flow is steady, laminar, and fully developed.

2. Analysis

2.1 Geometry

Heat sinks, used in microelectronics, usually consist of arrays of pin-fins arranged in an in-line or staggered manner as shown in Figs. 1 and 2. The pins are attached to a common base and the geometry of the array is determined by the pin dimensions, number of pins and pin arrangement.

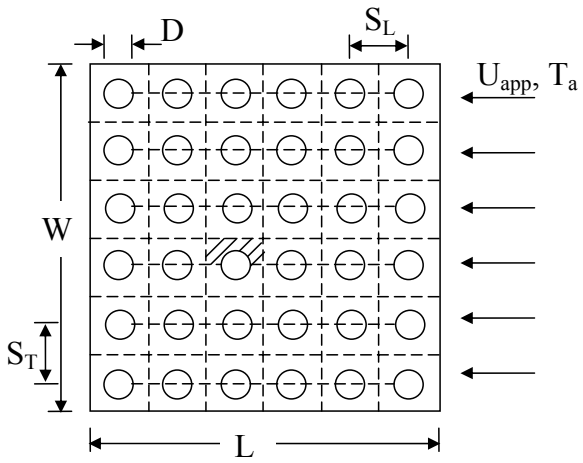

Figure 1 Schematic of In-Line Arrangement

The geometry of an in-line pin-fin heat sink is shown in Fig. 3. The dimensions of the baseplate are $L \times W \times t_b$, where L is the length in the streamwise direction, W is the width, and t_b is the thickness. Each pin fin has diameter D and height H. The longitudinal and transverse pitches are S_L and S_T respectively. The approach velocity of the air is U_{app}. The direction of the flow is parallel to the x-axis. The baseplate is kept at constant temperature $\overline{T}_b$ and the top surface ($y = H$) of the pins is adiabatic. The average local wall temperature of the pin surface is $\overline{T}_w(x)$. The heat source is idealized as a constant heat flux boundary condition at the bottom surface of the baseplate. The mean temperature of the heat source is $\overline{T}_s$. It is assumed that the heat sink is fully shrouded and the heat source is situated at the center of the baseplate.

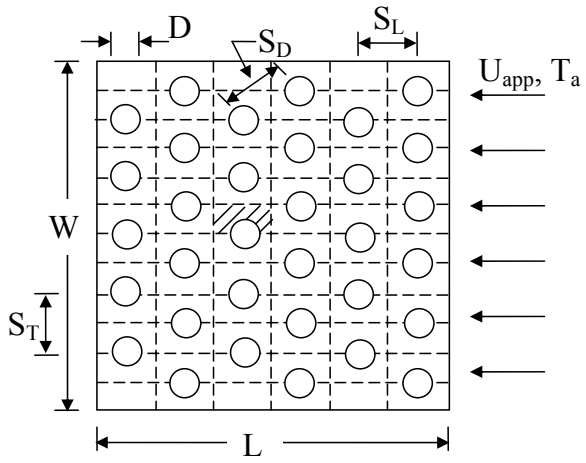

Figure 2 Schematic of Staggered Arrangement

It is assumed that the fluid temperature is averaged over the height of the heat sink, with $\overline{T}_f = \overline{T}_f(x)$, so the fluid temperature $\overline{T}_f(x)$ is the bulk mean fluid temperature. Fully developed heat and fluid flow are assumed in the analysis, and the thermophysical properties are taken to be temperature independent.

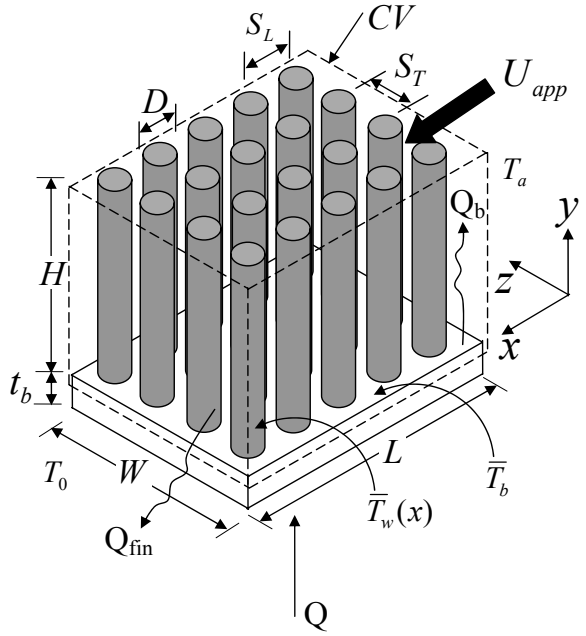

Figure 3 Geometry of In-Line Pin-Fin Heat Sink

2.2 Boundary Conditions

The boundary conditions for the heat sink under consideration can be specified as follows. For the hydrodynamic boundary conditions, the velocity is zero at all boundaries of the pins except the inlet and outlet. A uniform approach velocity U_{app} is applied at the inlet:

$$u = U_{app}, \quad v = 0, \quad w = 0|_{x=0,\ 0\le y\le H,\ 0\le z\le W} \tag{1}$$

For the thermal boundary conditions, adiabatic boundary conditions are applied to all boundaries except the heat sink baseplate. At the inlet, the fluid temperature is equal to the ambient temperature, that is

$$T = T_a|_{x=0,\ 0\le y\le H,\ 0\le z\le W} \tag{2}$$

whereas, at the exit,

$$T = T_0|_{x=L,\ 0\le y\le H,\ 0\le z\le W} \tag{3}$$

2.3 Reference Velocity

The mean velocity in the minimum free cross section between two rows, U_{max}, is used as a reference velocity in the calculations of fluid flow and heat transfer for both types of arrangements, and is given by:

$$U_{max} = max\left(\frac{\mathcal{S}_T}{\mathcal{S}_T - 1}U_{app}, \frac{\mathcal{S}_T}{\mathcal{S}_D - 1}U_{app}\right) \tag{4}$$

where U_{app} is the approach velocity, $\mathcal{S}_L$, and $\mathcal{S}_T$ are the dimensionless longitudinal and transverse pitches, and $\mathcal{S}_D = \sqrt{\mathcal{S}_L^2 + (\mathcal{S}_T/2)^2}$ is the dimensionless diagonal pitch in the case of a staggered arrangement.

2.4 Average Heat Transfer Coefficient for Heat Sink

If the base temperature of the heat sink $\overline{T}_b$ is averaged and assumed to be constant, the energy balance for the control volume (Fig. 3) is

$$Q = NQ_{fin} + Q_b \tag{5}$$

where

$$Q = (hA)_{hs}\ \theta_b \tag{6}$$

$$Q_{fin} = (Ah\eta)_{fin}\ \theta_b \tag{7}$$

$$Q_b = (hA)_b\,\theta_b \tag{8}$$

with

$$A_{hs} = NA_{fin} + \left(LW - N\frac{\pi D^2}{4}\right) \tag{9}$$

$$A_{fin} = \pi DH \tag{10}$$

$$A_b = LW - N\frac{\pi D^2}{4} \tag{11}$$

$$\eta_{fin} = \frac{\tanh(mH)}{mH} \tag{12}$$

$$m = \sqrt{\frac{4h_{fin}}{kD}} \tag{13}$$

$$N = N_L N_T \tag{14}$$

$$\theta_b = \overline{T}_b - T_a \tag{15}$$

The mean heat transfer coefficients h_{fin} and h_b for the baseplate and the pin-fin arrays are obtained by Khan [32] and are written as

$$h_b = \frac{0.75k_f}{D}\sqrt{\frac{\mathcal{S}_T - 1}{N_L\mathcal{S}_L\mathcal{S}_T}}Re_D^{1/2}Pr^{1/3} \tag{16}$$

$$h_{fin} = \frac{C_1k_f}{D}Re_D^{1/2}Pr^{1/3} \tag{17}$$

where C_1 is a constant which depends upon the longitudinal and transverse pitches, arrangement of the pins, and thermal boundary conditions. For isothermal boundary condition, it is given by

$$C_1 = [0.2 + \exp(-0.55\mathcal{S}_L)]{\mathcal{S}_T}^{0.285}{\mathcal{S}_L}^{0.212} \quad (18a)$$

for in-line arrangement, and

$$C_1 = \frac{0.61\,{\mathcal{S}_T}^{0.091}{\mathcal{S}_L}^{0.053}}{[1 - 2\exp(-1.09\,\mathcal{S}_L)]} \quad (18b)$$

for staggered arrangement.

Combining Eqs. (6)-(17), Eq. (5) can be solved for the average heat transfer coefficient of the heat sink

$$h_{hs} = C_2 \frac{k_f}{D} Re_D^{1/2} Pr^{1/3} \quad (19)$$

where C_2 is a constant and for both pin-fin arrangements, it is written as:

$$C_2 = \frac{C_1 \pi \gamma \eta_{fin} + 0.75\sqrt{\frac{\mathcal{S}_T - 1}{N_L \mathcal{S}_L \mathcal{S}_T}}\left(\mathcal{S}_T \mathcal{S}_L - \frac{\pi}{4}\right)}{\pi(\gamma - 1/4) + \mathcal{S}_T \mathcal{S}_L} \quad (20)$$

and $\gamma = H/D$ is the aspect ratio of the fin. Thus the dimensionless heat transfer coefficient for the heat sink may be expressed as

$$Nu_{D_{hs}} = \frac{h_{hs} D}{k_f} = C_2 Re_D^{1/2} Pr^{1/3} \quad (21)$$

2.5 Average Fluid Temperature

An energy balance for the control volume of length Δx (Fig. 4) gives

$$\dot{m} c_p [T_f(x + \Delta x) - T_f(x)] = dQ \quad (22)$$

where $\dot{m}$ is the mass flow rate of air and dQ is the heat flow coming from the fin and the exposed (unfinned) surface of the baseplate and they are given by:

$$\dot{m} = \rho U_{app} N_T S_T H \quad (23)$$

$$dQ = dQ_{fin} + dQ_b \quad (24)$$

Equation (22) can be simplified and integrated to give the fluid temperature $T_f(x)$ at any position inside the heat sink.

$$T_f(x) = \overline{T}_b - (\overline{T}_b - T_a) \cdot \exp\left[-\frac{(hA)_{hs}}{\dot{m} c_p} \cdot \left(\frac{x}{L}\right)\right] \quad (25)$$

Therefore, the average fluid temperature inside the heat sink will be

$$\overline{T}_f = \overline{T}_b - (\overline{T}_b - T_a)\left[\frac{\dot{m} c_p}{(hA)_{hs}}\right] \cdot \left[1 - \exp\left(-\frac{(hA)_{hs}}{\dot{m} c_p}\right)\right] \quad (26)$$

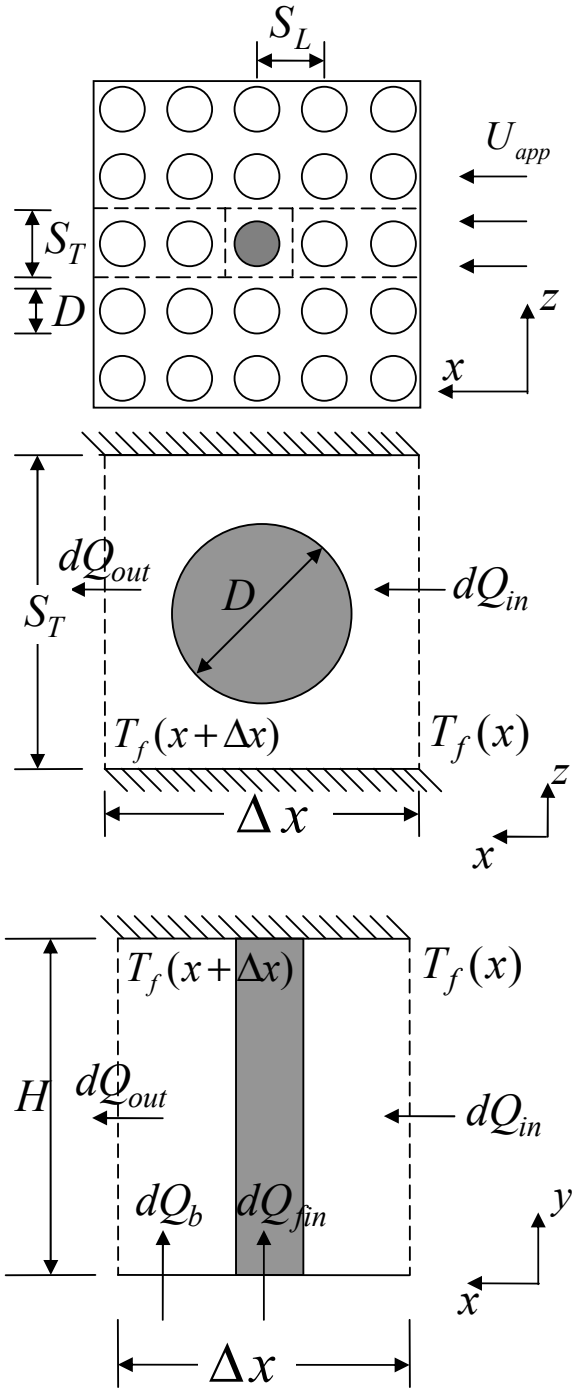

Figure 4 Control Volume for Energy Balance

The air temperature leaving the heat sink can be determined from Eq. (25) by using $T_f(x) = T_0$ at $x = L$:

$$T_o = \overline{T}_b - (\overline{T}_b - T_a) \cdot \exp\left[-\frac{(hA)_{hs}}{\dot{m} c_p}\right] \quad (27)$$

2.6 Heat Sink Resistance

Assuming that the entire baseplate is fully covered with electronic components, and the fins are machined

as an integral part of the baseplate, the thermal resistance of the heat sink can be written as

$$R_{th} = \frac{1}{\frac{N}{R_{fin}} + \frac{1}{R_b}} + R_m \quad (28)$$

where N is the total number of pin-fins, R_{fin} is the thermal resistance of the fin and is given by

$$R_{fin} = \frac{1}{(hA\eta)_{fin}} \quad (29)$$

R_b is the thermal resistance of the exposed surface of the baseplate, i.e.,

$$R_b = \frac{1}{h_b\left(LW - N\frac{\pi D^2}{4}\right)} \quad (30)$$

and R_m is the bulk resistance of the baseplate material and is given by

$$R_m = \frac{t_b}{kLW} \quad (31)$$

where k is the thermal conductivity of the baseplate, h_b and h_{fin} are the mean heat transfer coefficients for the fin array and the baseplate and can be determined from Eqs. (16) and (17) respectively.

2.7 Heat Sink Pressure Drop

For a heat sink, the total pressure drop is given by

$$\Delta P_{tot} = \Delta P_{1-a} + \Delta P_{a-b} + \Delta P_{b-2} \quad (32)$$

where ΔP_{1-a} is the pressure drop due to the irreversible free expansion that always follows the abrupt contraction, ΔP_{a-b} is the pressure loss due to core friction, and ΔP_{b-2} is the pressure loss associated with the irreversible free expansion and momentum changes following an abrupt expansion. These pressure drops can be written as:

$$\Delta P_{1-a} = k_c \cdot \frac{\rho U_{max}^2}{2} \quad (33)$$

$$\Delta P_{b-2} = k_e \cdot \frac{\rho U_{max}^2}{2} \quad (34)$$

$$\Delta P_{a-b} = fN_L \cdot \frac{\rho U_{max}^2}{2} \quad (35)$$

where k_c and k_e are the abrupt contraction and abrupt expansion coefficients respectively, f is the friction factor, and N_L is the number of pins in the longitudinal direction. The coefficients of abrupt contraction and expansion have been established graphically by Kays [33] for a number of geometries. The following correlations are derived from those graphs:

$$k_c = -0.0311\sigma^2 - .3722\sigma + 1.0676 \quad (36)$$

$$k_e = 0.9301\sigma^2 - 2.5746\sigma + 0.973 \quad (37)$$

with

$$\sigma = \frac{\mathcal{S}_T - 1}{\mathcal{S}_T} \quad (38)$$

Žukauskas and Ulinskas [10] collected data, from a variety of sources, about friction factors for the flow through in-line and staggered arrays having many rows and plotted them in the form Eu/K_1 versus Re_D, where Eu is the dimensionless pressure drop and K_1 is a parameter accounting for geometry. They fitted these plots by inverse power series relationships and recommended several correlations depending on of $\mathcal{S}_\mathcal{L}$, $\mathcal{S}_\mathcal{T}$ and Re_D. They also fitted and recommended several correlations for the correction factors for the pressure drop with small number of rows. These authors combined all the recommended correlations for pressure drop and their correction factors separately and developed single correlations for the friction factors and correction factors for each arrangement. These correlations can be used for any pitch and Reynolds number in the laminar flow range. They are given by

$$f = K_1\left[0.233 + 45.78/(\mathcal{S}_T - 1)^{1.1}Re_D\right] \quad (39a)$$

for in-line arrangement, and

$$f = K_1\left[378.6/\mathcal{S}_T^{13.1/\mathcal{S}_T}\right]/Re_D^{0.68/\mathcal{S}_T^{1.29}} \quad (39b)$$

for staggered arrangement. K_1 is a correction factor depending upon the flow geometry and arrangement of the pins. It is given by

$$K_1 = 1.009\left(\frac{\mathcal{S}_T - 1}{\mathcal{S}_L - 1}\right)^{1.09/Re_D^{0.0553}} \quad (40a)$$

for in-line arrangement, and

$$K_1 = 1.175(\mathcal{S}_L/\mathcal{S}_T Re_D^{0.3124}) + 0.5Re_D^{0.0807} \quad (40b)$$

for staggered arrangement.

3. Results and Discussion

The dimensions given in Table 1 are used as the default case for the modeling of both in-line and staggered pin-fin heat sinks. The air properties are evaluated at the ambient temperature. The results obtained for both in-line and staggered arrangements are shown in Table 2. It is clear from Table 2 that the in-line arrangement gives higher heat sink resistance and lower pressure drop than the staggered arrangement. As a result, the average heat transfer coefficient is lower and the baseplate temperature is higher for the in-line arrangement. It means that, under the same situation, staggered arrangement gives better thermal performance at the cost of higher pressure drop.

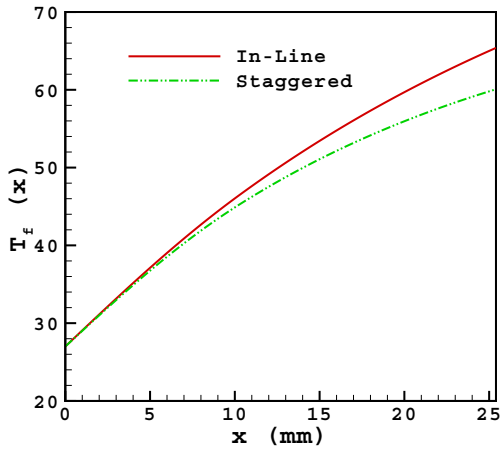

Figure 5 Temperature Distribution of Air in Pin-Fin Heat Sink

Figure 5 shows the temperature distributions of air in the heat sink for both arrangements. The baseplate is kept at constant temperature $\overline{T}_b$. No appreciable effect of pin-fin arrangements on the temperature of air could be found in the entrance region. However, as the distance from the inlet increases, the in-line arrangement shows higher temperature up to the exit. This is mainly due to higher thermal resistance offered by in-line arrangement.

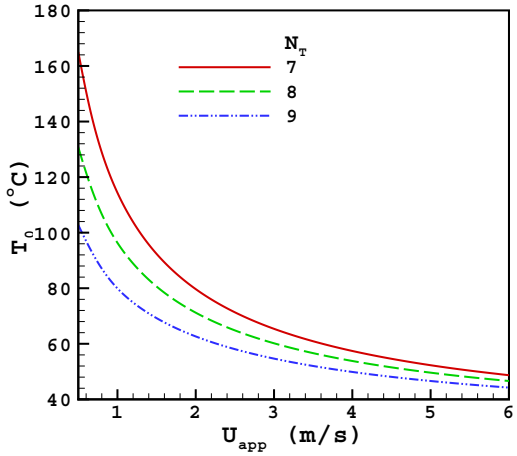

Figure 6 Temperature of Air Leaving Heat Sink as Function of U_{app} and N_T

The variation of air temperature at the exit versus approach velocity for different number of pins N_T in the in-line arrangement is shown in Fig. 6. As expected, the temperature of the air leaving the heat sink decreases with increasing approach velocity and number of transverse rows. As number of pins increases, the heat transfer surface area increases and as a result the temperature of the air decreases. The same behavior can be observed for staggered arrangement.

Figure 7 shows the total pressure drop versus approach velocity for different pin diameters in an in-line arrangement. The pressure drop increases with approach velocity and pin diameter. For small approach velocities and pin diameters, there is no appreciable change in the pressure drop. However, as the approach velocity and the pin diameter increase, the difference in pressure drops increase.

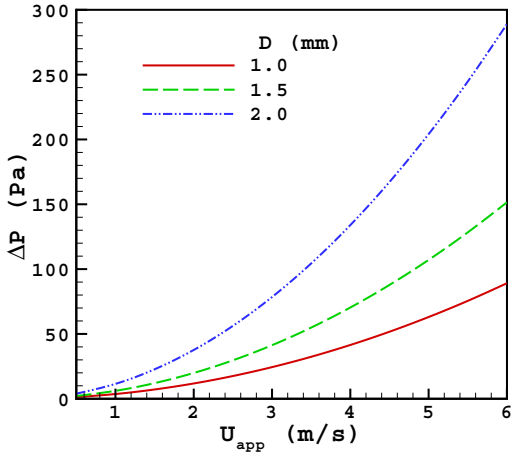

Figure 7 Pressure Drop as Function of U_{app} and D

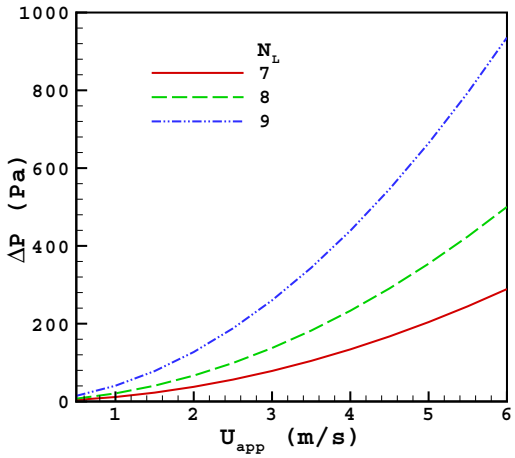

Figure 8 Pressure Drop as Function of U_{app} and N_L

Figure 8 shows the same trend of pressure drop for different number of pins in the flow direction. In both cases, whether pin diameter or number of pins increase, hydraulic resistance increases and as a result the pressure drop increases.

Table 1: Dimensions Used for Modeling of Pin-Fin Heat Sinks

Quantity	Dimension
Footprint (mm^2)	25.4×25.4
Heat Source Dimensions (mm^2)	25.4×25.4
Baseplate Thickness (mm)	2
Pin Diameter (mm)	2
Overall Height of Heat Sink (mm)	12
Number of Pins (In-Line) $N_T \times N_L$	7×7
Number of Pins (Staggered) $N_T \times N_L$	8×7
Approach Velocity (m/s)	3
Thermal Conductivity of Solid ($W/m \cdot K$)	180
Thermal Conductivity of Air ($W/m \cdot K$)	0.026
Density of Air (kg/m^3)	1.1614
Specific Heat of Air ($J/kg \cdot K$)	1007
Kinematic Viscosity (m^2/s)	1.58×10^{-5}
Prandtl Number (Air)	0.71
Heat Load (W)	50
Ambient Temperature (^0C)	27

Table 2: Results of In-Line and Staggered Heat Sinks

Quantity	In-Line	Staggered
Thermal Resistance ($^0C/W$)	1.35	0.94
Average Heat Transfer Coefficient ($W/m^2 \cdot K$)	210.7	271.8
Pressure Drop (Pa)	78.5	211.9
Average Fluid Temperature (^0C)	48.9	46.8
Average Baseplate Temperature (^0C)	94.3	74.0
Air Temperature Leaving Heat Sink (^0C)	65.4	60.1

Heat transfer from heat sinks depends mainly on the approach velocity, pin arrangement, heat sink material, and properties of the incoming fluid. Dimensionless heat transfer coefficients for the heat sink are plotted in Figs. 9-12 versus approach velocities. In Fig. 9, heat transfer coefficients are plotted for different pin diameters. The heat transfer coefficients of the heat sink increase rapidly with the pin diameter. For the specified baseplate dimensions, the increase in pin diameter decreases the transverse as well as longitudinal pitches which increases the heat transfer.

Figure 10 shows the variation of Nusselt number versus approach velocity for different pin heights. It is evident that heat transfer decreases with the increase in pin height but increases with approach velocity. With increasing number of transverse or longitudinal rows, heat transfer also increases. This is shown in Fig. 11. In Fig. 12, the variation of heat transfer coefficients is shown for different materials (having low thermal conductivity to high conductivity). It is clear that plastic composites ($k = 25W/m \cdot K$) have very low heat transfer coefficients, whereas aluminum and copper ($k = 180$ and $400W/m \cdot K$) have higher heat transfer coefficients. For higher approach velocities, the difference in heat transfer between these materials is also evident. The comparison of the present results with experimental/numerical data is presented in Figs. 12 and 13 for staggered arrangements. Present results are compared with the numerical results of Hamilton et. al (2002) and experimental correlation of Tahat et. al (1994). Good agreement can be seen in both figures.

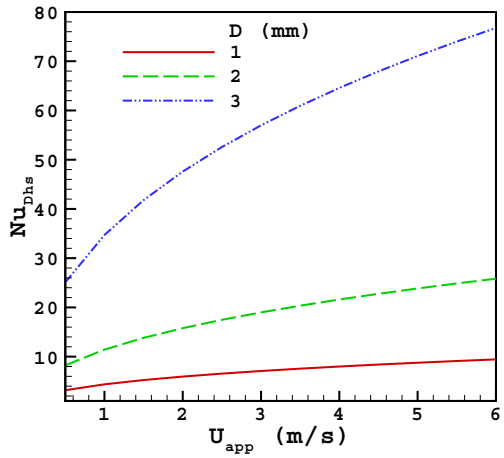

Figure 9 Nusselt Number as Function of U_{app} and D

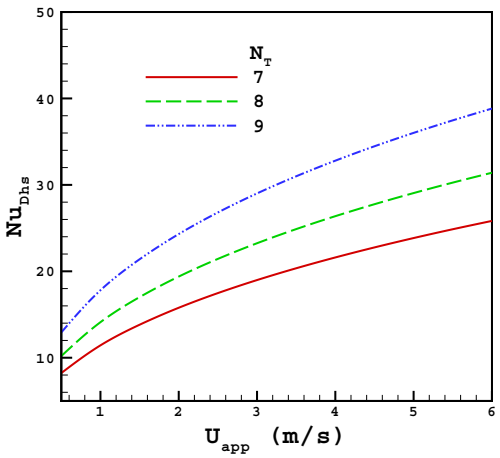

Figure 11 Nusselt Number as Function of U_{app} and N_T

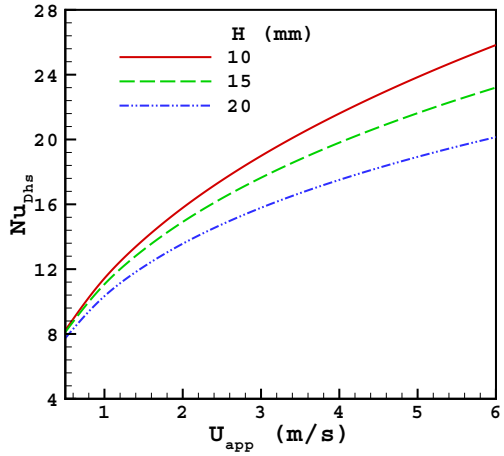

Figure 10 Nusselt Number as Function of U_{app} and H

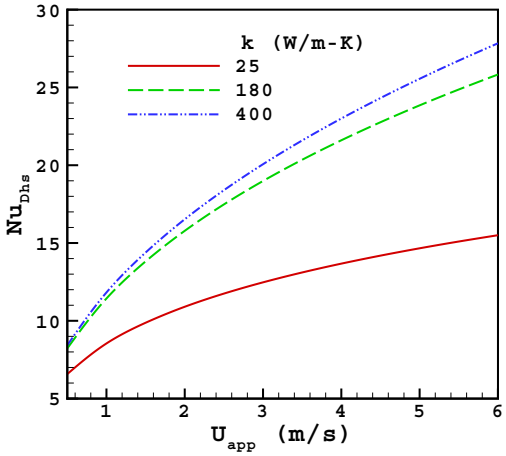

Figure 12 Nusselt Number as Function of U_{app} and k

4. Conclusions

1. Heat transfer from and pressure drop across the heat sink increases with the increase in approach velocity, pin diameter, and number of pins. Heat transfer also increases with the thermal conductivity of the material and with the pin height.

2. In-line arrangement gives higher heat sink resistance and lower pressure drop than the staggered arrangement.

3. Heat transfer models for in-line and staggered arrangements are suitable in designing pin-fin heat sinks.

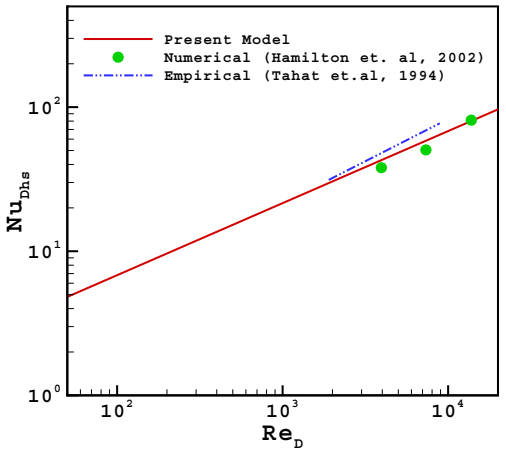

Figure 13 Nusselt Number as Function of Re_D for 2.5×1.5 Staggered Arrangement

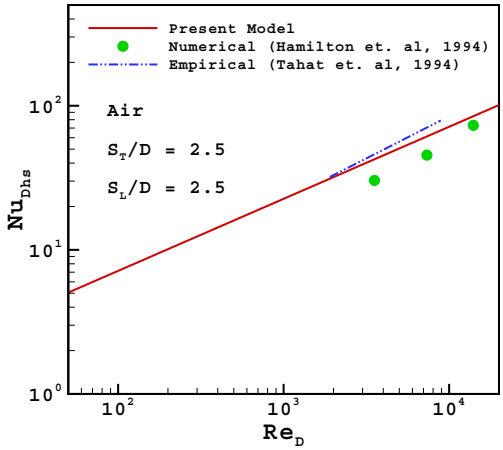

Figure 14 Nusselt Number as Function of Re_D for 2.5×2.5 Staggered Arrangement

Acknowledgments

The authors gratefully acknowledge the financial support of Natural Sciences and Engineering Research Council of Canada and the Center for Microelectronics Assembly and Packaging.

References

1. Chilton, T. H. and Genereaux, R. P., "Pressure Drop Across Tube Banks," Transactions of the American Institute of Chemical Engineers, Vol. 29, pp. 161-173, 1933.
2. Grimison, E. D., "Correlation and Utilization of New Data on Flow Resistance and Heat Transfer for Cross Flow of Gases over Tube Banks," Transactions of ASME, Vol. 59, pp. 583-594, 1937.
3. Jakob, M., "Heat Transfer and Flow Resistance in Cross Flow of Gases Over Tube Banks," ASME Journal of Heat Transfer, Vol. 60, pp. 384-386, 1938.
4. Gunter, A. Y. and Shaw, W. A., "A General Correlation of Friction Factors for Various Types of Surfaces in Crossflow," Transactions of ASME, Vol. 67, pp. 643-660, 1945.
5. Bergelin, O. P., Brown, G. A., Hull, H. L., and Sullivan, F. W., "Heat Transfer and Fluid Friction During Flow Across Banks of Tubes - III: A Study of Tube Spacing and Tube Size," ASME Journal of Heat Transfer, Vol. 72, pp. 881-888, 1950.
6. Norris, R. H. and Spofford, W. A., "High Performance Fins for Heat Transfer," Transactions of ASME, Vol. 64, pp. 489-496, 1942.
7. Huge, E. C., "Experimental Investigation of Effects of Equipment Size on Convection Heat Transfer and Flow Resistance in Cross Flow of Gases Over Tube Banks" Transactions of ASME, Vol. 59, pp. 573-581, 1937.
8. Pierson, O. L., "Experimental Investigation of the Influence of Tube Arrangement on Convection Heat Transfer and Flow Resistance in Cross Flow of Gases Over Tube Banks," Transactions of ASME, Vol. 59, pp. 563-572, 1937.
9. Wallis, R. P. and White, C. M., "Resistance to Flow Through Nests of Tubes," Transactions of ASME, Vol. 59, pp. 583-594, 1938.
10. Žukauskas, A. and Ulinskas, R., "Heat Transfer in Tube Banks in Crossflow," Hemisphere, Washington, DC, 1988.
11. Dvinsky, A., Bar-Cohen, A. and Strelets, M., "Thermofluid Analysis of Staggered and In-line Pin Fin Heat Sinks," The Seventh Inter Society Conference on Thermal Phenomena, Las Vegas, Nevada, USA, May 23 - 26, Vol. 1, pp. 157-164, 2000.
12. Jung, H. H. and Maveety, J. G., "Pin Fin Heat Sink Modeling and Characterization," Sixteenth IEEE Semi-Therm Symposium, San Jose, CA USA, March 21 -23, pp. 260-265, 2000.
13. You, H. I. and Chang, C. H., "Numerical Prediction of Heat Transfer Coefficient for a Pin-Fin Channel Flow," Journal of Heat Transfer, Vol. 119, November, pp. 840-843, 1997.
14. Wang, W. and Sangani, A. S., "Nusselt Number for Flow Perpendicular to Arrays of Cylinders in the Limit of Small Reynolds and Large Peclet Numbers," Physics of Fluids, Vol. 9, No. 6, pp. 1529-1539, 1997.
15. Wung, T. S. and Chen, C. J., "Finite Analytic Solution of Convective Heat Transfer For Tube Arrays in Crossflow: Part I - Flow Field Analysis," ASME Journal of Heat Transfer, Vol. 111, August, pp. 633-640, 1989.
16. Tahat, M. A., Kodah, Z. H., Jarrah, B. A. and Probert, S. D., "Heat Transfer from Pin-Fin Arrays Experiencing Forced Convection," Applied Energy, Vol. 67, pp. 419-442, 2000.
17. Tahat, M. A., Babus'Haq, R. F., and Probert, S. D., "Forced Steady-State Convections from Pin Fin Arrays," Applied Energy, Vol. 48, pp. 335-351, 1994.
18. Maudgal, V. K., and Sunderland, J. E., "Forced Convection Heat Transfer from Staggered Pin Fin Arrays," 31st National Heat Transfer Conference, Vol. 7, Houston, Texas, August 3-6, pp. 35-44, 1996.
19. Wirtz, R. A., Sohal, R., and Wang, H., "Thermal Performance of Pin-Fin Fan-Sink Assemblies," J. of Electronic Packaging, Vol. 119, March, pp. 26-31, 1997.
20. Babus'Haq, R. F., Akintunde, K. and Probert, S. D., "Thermal Performance of a Pin-Fin Assembly," Int. J. of Heat and Fluid Flow, Vol. 16, No. 1, pp. 50-55, 1995.

21. Azar, K. and Mandrone, C. D., "Effect of Pin Fin Density of the Thermal Performance of Unshrouded Pin Fin Heat Sinks," ASME Journal of Electronic Packaging, Vol. 116, pp. 306-309, 1994.
22. Minakami, K. and Iwasaki, H., "Heat-Transfer Characteristics of Pin-Fins with In-Line Arrangement," Heat Transfer - Japanese Research, Vol. 23, No. 3, pp. 213-228, 1994.
23. Vanfossen, G. J., "Heat Transfer Coefficients for Staggered Arrays of Short Pin Fins," ASME Journal of Engineering for Power, Vol. 104, pp. 268-274, 1982.
24. Metzger, D. E., Berry, R. A., and Bronson, J. P., "Developing Heat Transfer in Rectangular Ducts With Staggered Arrays of Short Pin Fins," ASME Journal of Heat Transfer, Vol. 104, pp. 700-706, 1982.
25. Metzger, D. E., Fan, Z. X., and Shepard, W. B., "Pressure Loss and Heat Transfer Through Multiple Rows of Short pin Fins," Heat Transfer 1982, Vol. 3, Grigull et al. Editors, Hemisphere, Washington, pp. 137-142, 1982.
26. Metzger, D. E., Fan, C. S., and Haley, S. W., "Effects of Pin Shape and Array Orientation on Heat Transfer and Pressure Loss in Pin Fin Arrays," ASME Journal of Heat Transfer, Vol. 106, pp. 252-257, 1984.
27. Armstrong, J. and Winstanley, D., "A Review of Staggered Array Pin Fin Heat Transfer for Turbine Cooling Applications," ASME Journal of Turbomachinery, Vol. 110, pp. 94-103, 1988.
28. Hamilton, H. J., Adametz, D. S., Lind, E. K., and Gopinath, A., "Numerical Analysis of the Performance of a Staggered Cross-Pin Array Heat Exchanger," AIAA 2002-3008, 8th AIAA/ASME Joint Thermophysics and Heat Transfer Conference, 24-26 June, 2002, St. Louis, Missouri.
29. Holman, J. P., "Heat Transfer," McGraw-Hill Book Company, New York, 7th Edition, pp. 307-310, 1992.
30. Kreith, F, and Bohn, M. S., "Principles of Heat Transfer," West Publishing Company, New York, 5th Edition, pp. 469-485, 1993.
31. Incropera, F. P. and DeWitt, D. P., "Introduction to Heat Transfer," John Wiley & Sons, Inc., New York, 2002.
32. Khan, W. A., 2004, "Modeling of Fluid Flow and Heat Transfer for Optimization of Pin-Fin Heat Sinks," Ph. D. Thesis, Department of Mechanical Engineering, University of Waterloo, Canada.
33. Kays, W. M., "Loss Coefficients for Abrupt Changes in Flow Cross Section With Low Reynolds Number Flow in Single and Multiple Tube Systems," Transactions of ASME, November, pp. 1067-1074, 1950.